

Flavor blocking of dark matter thermalization in neutron stars

Hooman Davoudiasl,^{1,*} Jaime Hoefken Zink,^{2,†} and Sebastian Trojanowski^{2,3,‡}

¹*High Energy Theory Group, Physics Department,
Brookhaven National Laboratory, Upton, NY 11973, USA*

²*National Centre for Nuclear Research, Pasteura 7, Warsaw, PL-02-093, Poland*

³*Astrocent, Nicolaus Copernicus Astronomical Center Polish Academy of Sciences, ul. Rektorska 4, 00-614, Warsaw, Poland*
(Dated: November 27, 2025)

Neutron stars (NSs) provide exceptional laboratories for probing dark matter (DM) interactions beyond the reach of terrestrial experiments. We investigate a scenario in which DM couples to electrons and muons through a lepton-flavor-violating (LFV) coupling. In the strong gravitational field of NSs, infalling DM attains semi-relativistic velocities that activate inelastic transitions $\chi e \leftrightarrow \chi \mu$, leading to efficient energy deposition through scattering and annihilation. We show that this latter heating mechanism remains efficient even for p -wave suppressed annihilations. This is due to *flavor blocking* of DM thermalization with the NS, as LFV interactions become forbidden for low kinetic energies of χ . The resulting DM-induced heating can sustain NS surface temperatures of $T_s \gtrsim 2 \times 10^3$ K, providing an observable signature for future infrared searches. This establishes NS heating as a powerful probe of flavor-violating DM portals, capable of probing thermal targets beyond the reach of direct, indirect, and accelerator-based searches, as we illustrate for the axion-like particle (ALP) mediator.

Introduction: The microscopic nature and origin of dark matter (DM) remain unknown. The leading hypothesis is that DM was produced in thermal equilibrium in the early, radiation-dominated universe. This paradigm of thermal DM production has motivated numerous experimental efforts, with current and next-generation DM detectors aiming to explore this possibility fully [1, 2]. To achieve this goal, it is essential to consider both traditional DM searches and to look beyond them [3]. Astrophysical signatures play a key role in this endeavor, particularly for beyond the Standard Model (BSM) scenarios that are otherwise difficult to probe [4].

Neutron stars (NSs) have been recognized as a particularly compelling laboratory to test DM interactions. Observations of old and cold NSs could allow for constraining DM-nucleon scattering cross sections as low as $\sigma_{\chi N} \sim 10^{-45}$ cm² through expected DM-induced NS heating [5–27] or excessive DM accretion leading to NS collapse and black hole formation [28–31]. DM-lepton couplings can be similarly probed [32–35], taking advantage of the expected large number densities of both electrons and muons in NS interiors [36]. The presence of the latter, in particular, offers unique capabilities to probe DM couplings to muons [37].

In this study, we analyze for the first time the impact of possible lepton flavor violation (LFV) in DM couplings on NS heating, specifically a DM-DM- $e\mu$ interaction. We note that this scenario remains beyond the reach of traditional DM direct detection (DD) searches. However, in the strong gravitational field of the NS, the DM particle is boosted, and the electron gas gains a non-zero chemical potential, which enables $\chi e \rightarrow \chi \mu$ upscattering. Furthermore, DM particles can interact with muons in the NS interior, leading to an additional scattering mode, $\chi \mu \rightarrow \chi e$, which is inaccessible in terrestrial searches. In-

stead, elastic scatterings off electrons, $\chi e \rightarrow \chi e$, are only loop-induced in this case and remain strongly suppressed.

The NS heating by DM proceeds through two main mechanisms: the deposition of DM kinetic energy gained from the NS’s strong gravitational field, and subsequent DM annihilations within the star’s interior. The latter process can deposit energy equivalent to the entire rest mass of the DM particle, making it a more efficient heating mechanism. If the annihilation cross section is high enough, this process could also be independently confirmed by indirect detection (ID) observations of DM.

As we will discuss, the kinematics of inelastic scattering off leptonic targets prevent LFV DM from reaching thermal equilibrium with the NS temperature. The higher DM temperature inside the NS fuels efficient annihilation heating, even in the case of p -wave suppressed annihilations. This allows for probing thermal relic targets beyond the reach of DD and ID searches.

We illustrate this using a sample portal between the visible and dark sectors, which involves light axion-like particles (ALPs) [38–40]. ALPs can naturally emerge as pseudo-Nambu-Goldstone bosons from global symmetries spontaneously broken at high energy scales. They can mediate interactions between DM and the Standard Model (SM). In this scenario, the complex dark sector manifests primarily through ALP-induced DM couplings at lower energies. ALP couplings need not respect the SM flavor structure and could even play a role in generating it, *e.g.*, through familons [41, 42] or flavons [43]. LFV couplings of ALPs can also be radiatively generated [44]. Therefore, they can naturally mediate LFV interactions of DM. We show that future observations of old NSs with temperatures around $T \sim 2000$ K will provide leading constraints on this scenario.

The LFV model: We assume that ALPs couple to the

SM predominantly through LFV interactions with muons and electrons,

$$\mathcal{L} \supset -ig_{e\mu} a \bar{e} [\sin \phi + \cos \phi \gamma^5] \mu + \text{h.c.} \quad (1)$$

In the following, we will consider a purely pseudoscalar coupling by setting $\phi = 0$. We note that the precise value of this angle plays a minor role in the semi-relativistic regime of scattering within NSs.

Such LFV couplings can be inherited from the interactions of new heavy fields at a scale Λ , such that $g_{\mu e} = C_{\mu e} m_\mu / \Lambda$ and $C_{\mu e} \sim 1$ [45]. Requiring that these new fields be accessible at colliders, *i.e.*, $\Lambda \lesssim 10$ TeV, provides a target of $g_{\mu e} \gtrsim 10^{-5}$, which can only be partially probed in future ALP searches [46, 47]. Testing even lower couplings requires more indirect probes. In particular, the couplings in eq. (1) can induce rare muon decay rates far exceeding SM predictions. However, for ALP masses $m_a > m_\mu$, where m_μ is the mass of the muon, these bounds often require both LFV and lepton flavor conserving (LFC) couplings [48–50]. Exploring ALP scenarios where the LFC couplings are strongly suppressed is considerably more difficult and may necessitate novel experimental techniques [45, 51–61] or astrophysical probes [25, 50, 62–64].

We further introduce ALP couplings to DM, which we assume consists of a Dirac fermion χ ,

$$\mathcal{L} \supset -ig_\chi a \bar{\chi} \gamma^5 \chi. \quad (2)$$

Here, the dark coupling constant g_χ can be, *a priori*, unrelated to $g_{\mu e}$. However, the couplings can also exhibit a natural scaling, $g_\chi / g_{\mu e} \sim m_\chi / m_\mu$, provided that they originate from a common dark sector at the UV completion scale Λ .

If the dark coupling constant is not suppressed, $g_\chi \gg g_{\mu e}$, the DM relic density is determined by the dominant secluded annihilation mode, $\bar{\chi}\chi \rightarrow aa$. The corresponding cross section is given by [65]

$$\langle \sigma v \rangle_{aa} \simeq \frac{6}{x_{\text{f.o.}}} \frac{g_\chi^4}{24\pi} \frac{m_\chi^2 (m_\chi^2 - m_a^2)^2}{(2m_\chi^2 - m_a^2)^4} \left(1 - \frac{m_a^2}{m_\chi^2} \right)^{1/2}, \quad (3)$$

where $x_{\text{f.o.}} \equiv m_\chi / T_{\text{f.o.}}$, at freeze-out temperature $T_{\text{f.o.}}$. Here, requiring that the thermal DM abundance equals $\Omega_\chi^{\text{th}} h^2 \simeq 0.12$ [66] determines $g_{\chi, \text{th}}$ as a function of the dark sector masses. We apply this relationship when discussing the aforementioned benchmark scenario. This means that we assume $\Omega_\chi^{\text{th}} h^2 \simeq 0.12$, irrespective of the coupling to the SM leptons, $g_{\mu e}$. For our benchmark scenario, we find that $g_{\chi, \text{th}} \simeq 0.1 \sqrt{m_a / \text{GeV}} \gg g_{\mu e}$ within the allowed parameter space.

The aforementioned annihilation mode is *p*-wave suppressed. However, additional *s*-wave annihilations into SM leptons, $\bar{\chi}\chi \rightarrow \mu e$, are also possible. These remain subdominant in the early universe but can become comparable to or more efficient than secluded annihilations

at the present epoch, provided $g_{\mu e}$ is not too small. The relevant cross section is given by [45]

$$\langle \sigma v \rangle_{\mu e} \simeq \frac{g_{\mu e}^2 g_\chi^2}{16\pi} \frac{(4m_\chi^2 - m_\mu^2)^2}{m_\chi^2 (4m_\chi^2 - m_a^2)^2}. \quad (4)$$

This process introduces additional DM indirect detection (ID) bounds. As shown below, future observations of old NSs could yield significantly stronger constraints on $g_{\mu e}$, which are based on efficient *p*-wave annihilations of LFV DM particles inside NSs.

LFV dark matter capture: In the vicinity of the NS, DM particles are gravitationally attracted and boosted, leading to DM-induced heating due to their scatterings in the star and possible subsequent annihilations. The DM capture rate as seen by an observer far from the star is given by [15]

$$C = \frac{4\pi}{v_{\text{NS}}} \frac{\rho_\chi}{m_\chi} \text{Erf} \left(\sqrt{\frac{3}{2}} \frac{v_{\text{NS}}}{v_d} \right) \times \int_0^{R_{\text{NS}}} \sqrt{g_{rr}} r^2 \frac{\sqrt{1 - g_{tt}(r)}}{g_{tt}(r)} \Omega^-(r) \eta(r) dr, \quad (5)$$

where $v_{\text{NS}} = 230$ km/s is the NS velocity with respect to the local DM halo with the DM density of $\rho_\chi = 0.4$ GeV/cm³, $v_d = 270$ km/s is the DM velocity dispersion, assuming a Maxwell-Boltzmann distribution, and $g_{tt}(r)$ is the time component of the NS metric dependent on the position in the star, and $\sqrt{g_{rr}}$ is the square root of the radial component of the metric, which comes from the Jacobian of the volume integration. This last factor is usually forgotten. In NSs, g_{rr} can take values up to ~ 2 . The optical factor $\eta(r)$ accounts for the DM absorption within the NS. The interaction rate $\Omega^-(r)$ is the probability of DM scattering that reduces an outgoing χ 's speed below the local escape velocity at position r within the star, $v_e^2(r) = 1 - g_{tt}(r)$. These captured DM particles deposit their kinetic energy through subsequent scatterings, heating the NS. For relevant DM masses, a single scattering is typically sufficient for capture.

For LFV DM interactions, kinetic heating involves two interaction modes, such that $\Omega^- \equiv \Omega_{\mu \rightarrow e}^- + \Omega_{e \rightarrow \mu}^-$. DM particles entering the NS can first interact with electrons. The $\chi e \rightarrow \chi \mu$ upscattering becomes allowed at a radial distance $R_{\text{eff}} < R_{\text{NS}}$, where R_{NS} is the radius of the star. R_{eff} marks the position where the lepton chemical potential and density become sufficiently high to allow DM scattering off relativistic electron targets. At a slightly smaller radius, $R_\mu < R_{\text{eff}}$, muons are stable inside the NS, and the $\chi \mu \rightarrow \chi e$ scattering mode also becomes possible. Detailed expressions for the interaction rate and optical factor are provided in *Supplementary Material*.

In fig. 1, we present sample optical factors $\eta(r)$ as a function of radial position within an NS, for $m_\chi = 2$ GeV ($m_a = 1$ GeV) and selected values of the $g_{\mu e}$ coupling.

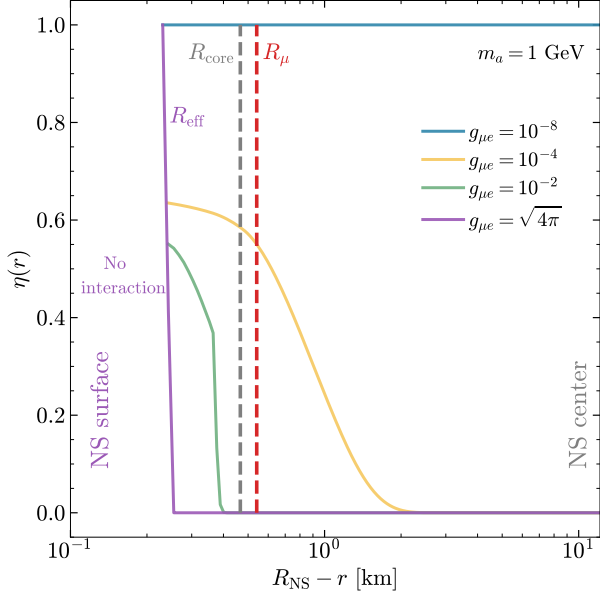


FIG. 1. Optical factor, $\eta(r)$, for a $2 M_\odot$ NS modeled with the BSk25 equation of state. We assume $m_\chi = 2 m_a$, $m_a = 1$ GeV, and the thermal value of $g_{\chi, \text{th}}$. Results are presented for selected $g_{\mu e}$ coupling strengths, as indicated. The purple-shaded region, corresponds to low values of $R_{\text{NS}} - r$, where R_{NS} is the NS radius and r is the distance measured from the center of the star. This region marks the regime close to the star's surface where the electron chemical potential and density are too low and their upscattering to muons in the outer NS crust can be neglected. R_μ denotes the radius of the stable muon region within the star. We indicate the transition between the crust and core of the star by a vertical gray dashed line. The center of the star is toward the right-hand side, where $R_{\text{NS}} - r \rightarrow 0$.

We assume an NS mass of $M_{\text{NS}} = 2 M_\odot$ and the BSk25 equation of state (EoS) [67–69], which yields a radius of $R_{\text{NS}} = 12.13$ km and central density of $\rho_c = 1.185 \times 10^{15}$ g/cm³. We also mark the position of the effective radius R_{eff} , relevant for this DM mass, and the muon radius R_μ in the core of the star.

As the figure illustrates, for large couplings, $\eta(r)$ approaches a naive geometric limit, indicating that most DM particles scatter close to the surface of the star at $r \approx R_{\text{eff}}$. This contrasts with the optically-thin regime, where $\eta(r) \sim 1$ for diminishing $g_{\mu e}$. In intermediate scenarios, DM particles penetrate deeper into the star, experiencing larger boost factors before interacting in the NS core.

We illustrate this with the yellow line in the plot, obtained for the limiting value of $g_{\mu e} = 10^{-4}$. The initial drop in $\eta(r)$ at $r \approx R_{\text{eff}}$ occurs due to partial attenuation of the DM flux as it passes through the NS interior before reaching position r . As we discuss below, larger values of $g_{\mu e}$ tend to be excluded by past searches. Hence, we expect DM particles in the considered BSM scenario to typically interact at $r < R_\mu$ and participate in both DM-

e and DM- μ scatterings.

NS heating: To quantify DM-induced heating, we evaluate the rate of kinetic energy E_k deposition in the NS considering both processes, $\chi(k_1) \ell_\alpha(p_1) \rightarrow \chi(k_2) \ell_\beta(p_2)$, where the 4-momenta are in parentheses and the Greek subscripts refer to the leptons involved, e and μ ,

$$\dot{E}_k = \frac{4\pi}{v_{\text{NS}}} \frac{\rho_\chi}{m_\chi} \text{Erf} \left(\sqrt{\frac{3}{2}} \frac{v_{\text{NS}}}{v_d} \right) \times \int_0^{R_{\text{NS}}} \sqrt{g_{rr}} r^2 \frac{\sqrt{1 - g_{tt}(r)}}{g_{tt}(r)} E_k^-(r) \eta(r) dr. \quad (6)$$

Here, $E_k^- \equiv (E_k^-)_{\mu \rightarrow e} + (E_k^-)_{e \rightarrow \mu}$, and

$$(E_k^-)_{\alpha \rightarrow \beta} = \frac{\zeta}{32\pi^3 m_\chi} \sqrt{\frac{g_{tt}}{1 - g_{tt}}} \times \int_{m_\alpha}^{\mu_l} dE_{p_1} E_{p_1} \int_{s_{\min}}^{s_{\max}} \frac{s ds}{g_s(m_\alpha) \beta_s(m_\alpha)} \times \int_{t_{\min}}^{t_{\max}} dt \langle |\mathcal{M}|^2 \rangle \gamma_s E_k \Theta(E_{p_2} - \mu_l), \quad (7)$$

where $g_s(m)$ and $\beta_s(m)$ are functions defined in the Supplemental Material, and $\gamma_s \equiv 1/\sqrt{g_{tt}(R_{\text{NS}})}$ is the boost factor on the surface, *i.e.*, the boost factor any particle would acquire when coming from rest far from the star to its surface. We note that we measure the energy deposition locally, as seen from the surface of the star, and the γ_s factor accounts for the relevant time dilation. This is included in Equation (6) to obtain the energy deposition from the expression for capture rate, since the latter (C) represents the amount of particles captured per second as measured far from the star. This rate is modified by gravity on the surface. The time dilation has been generally ignored in the literature, but we point out its importance for precise estimations.

For cold neutron stars, DM capture can be regarded as the only source of heating. The temperature on the star's surface then reads as follows [10]

$$T_s = \left(\frac{\dot{E}_k}{4\pi\sigma_{\text{SB}} R_{\text{NS}}^2} \right)^{1/4}, \quad (8)$$

where σ_{SB} is the Stefan-Boltzmann constant. Future telescope campaigns could reach the sensitivity to observe NSs with $\mathcal{O}(10^3 \text{ K})$ temperatures [10, 70].

DM particles interact with leptons in the star, depositing kinetic energy into it. If a DM particle loses all of its kinetic energy during an interaction at radius r inside the star, the equivalent kinetic energy deposition measured on the NS surface is given by $E_k^{\text{scat}} = \xi_r (\gamma_r - 1) m_\chi$. Here, $\xi_r \equiv \gamma_s / \gamma_r$ and γ_r is the boost factor at r . If DM particles deposit most of their kinetic energy close to the NS surface, we find $E_k^{\text{scat}} = (\gamma_s - 1) m_\chi$ [10]. As the DM particle continues to sink towards the center of the

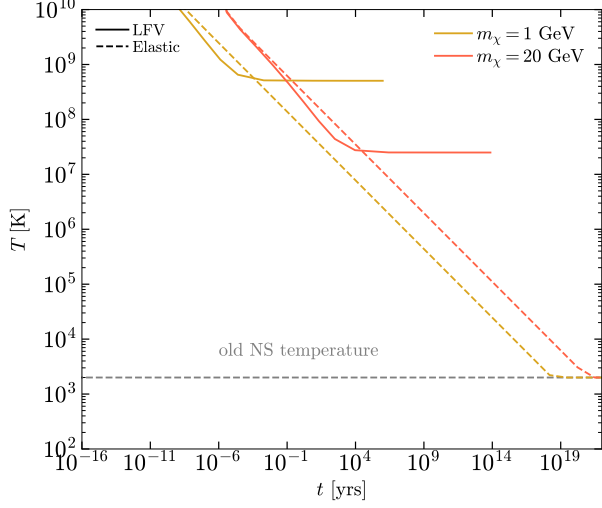


FIG. 2. Evolution of the DM temperature (T_{DM}) over time t in years for $m_\chi = 2 m_a$ and $m_\chi = 1$ GeV (brown lines) or 20 GeV (red). Solid lines correspond to LFV DM, while dashed lines represent the lepton flavor conserving case. The horizontal gray dashed line indicates the temperature of an old neutron star, T_{NS} .

star, it keeps depositing the excess kinetic energy it gains in this process [23]. In the *Supplementary Material*, we show that this additional, continued deposition can be approximately equivalent to considering the initial DM particle interaction to occur at the center of the star, such that $E_k^{\text{scat}} = \xi_0 (\gamma_0 - 1) m_\chi$.

Subsequent DM annihilations close to the NS center deposit additional energy in the star, given by $E_k^{\text{ann}} = f_{\text{ann}} \xi_0 m_\chi$. Here, $f_{\text{ann}} \equiv 2\Gamma_{\text{ann}}/C$ is the fraction of DM particles that annihilate relative to the capture rate. The annihilation rate, $\Gamma_{\text{ann}} = (1/2)A_\chi N_\chi^2$, depends on the number of DM particles in the star, N_χ . In the parameter space explored in this work, $f_{\text{ann}} = 1$ for an NS age of $t \geq 10^4$ yr. Therefore, we find the total kinetic energy deposition

$$E_k = E_k^{\text{scat}} + E_k^{\text{ann}} = \xi_0 \gamma_0 m_\chi = \gamma_s m_\chi. \quad (9)$$

The annihilation factor depends on the relevant cross section and the effective volume occupied by DM particles after they thermalize in the center of the star, $A_\chi \sim \langle \sigma_{\text{ann}} v \rangle / r_0^3$, where $r_0 = \sqrt{3T_{\text{DM}}/(2\pi G m_\chi \rho_c)}$. At late times and for elastic DM interactions, the DM is expected to eventually thermalize with the NS temperature, T_{NS} . However, this process can be prolonged for specific DM scenarios [17, 23]; see also the discussion on the partial thermalization of inelastic DM [71].

Here we point out that, when only LFV interactions are possible, the kinematics of inelastic scatterings with electron and muon targets in the star prevents DM from cooling below a threshold temperature. In the *Supplementary Material*, we show that for sufficiently small

DM kinetic energies, the minimum target lepton energy that renders LFV interactions possible is given by $E_{p_1}^+ = \Delta m_{\mu e}^2 / 2q$, where q is the three-momentum exchange and $\Delta m_{\mu e}^2 = m_\mu^2 - m_e^2$. This condition is most easily satisfied when $q = q_{\text{max}} \simeq 2\sqrt{3m_\chi T_{\text{DM}}}$, which corresponds to a back-scattering event. We then find $E_{p_1}^+ = \Delta m_{\mu e}^2 / 4\sqrt{3m_\chi T_{\text{DM}}}$. As can be seen, as the DM temperature T_{DM} decreases, the minimum required lepton energy $E_{p_1}^+$ can exceed the chemical potential close to the center of the star, $\mu \sim 250$ MeV, i.e. $E_{p_1}^+ > \mu$. At this point, the LFV interactions can no longer thermalize DM particles within the star, leading to the following lower limit for the DM temperature

$$T_{\text{DM}} \gtrsim \frac{1}{3m_\chi} \left(\frac{\Delta m_{\mu e}^2}{4\mu} \right)^2. \quad (10)$$

We illustrate the evolution of the DM temperature in fig. 2. In the plot, we compare this with the standard DM temperature evolution obtained when elastic (lepton flavor conserving) DM scattering off electron and muon targets is allowed. As can be seen, in the LFV case, DM rapidly equilibrates, but its temperature remains orders of magnitude higher than the NS temperature, $T_{\text{DM}} \gg T_{\text{NS}}$. Notably, for $m_\chi \sim \text{GeV}$, this temperature, $T_{\text{DM,NS}} \sim 43$ keV, also exceeds the characteristic DM temperature in the Milky Way (MW), $T_{\text{DM,MW}} \sim m_\chi v_\chi^2 \sim \text{keV}$ for $v_\chi \sim 10^{-3}$.

We note that, at very late times, DM is expected to fully thermalize with the star due to loop-induced processes, $\chi e \rightarrow \chi e$ and $\chi \mu \rightarrow \chi \mu$. These processes remain very strongly suppressed such that the relevant thermalization time significantly exceeds the age of the universe.

The increased DM temperature affects the interplay between the p -wave and s -wave annihilation modes inside the star because the annihilation factor varies differently with T_{DM} in both cases, $A_\chi \sim 1/T_{\text{DM}}^{n/2}$, where $n = 3$ for s -wave and $n = 1$ for p -wave. As a result, we find that for the allowed values of the $g_{\mu e}$ coupling and the values of the dark coupling constant g_χ corresponding to the thermal DM target, the annihilation heating of NSs for LFV interactions is driven by the p -wave process, $\chi\bar{\chi} \rightarrow aa$, due to the *flavor blocking* of DM thermalization in the star.

The produced ALPs deposit their energy by decaying back into $e^\pm \mu^\mp$ pairs. For ALP masses close to the kinematical threshold, $m_a \sim m_\mu + m_e$, such decays remain Pauli-blocked in the NS inner core, where the lepton chemical potential is high. In this case, ALPs travel to the outer region of the star, where the chemical potential decreases, and deposit their energy there, therefore still heating the star.

Discussion: In fig. 3, we illustrate the projected exclusion bounds on the considered LFV DM scenario that would result from future observations of NSs with tem-

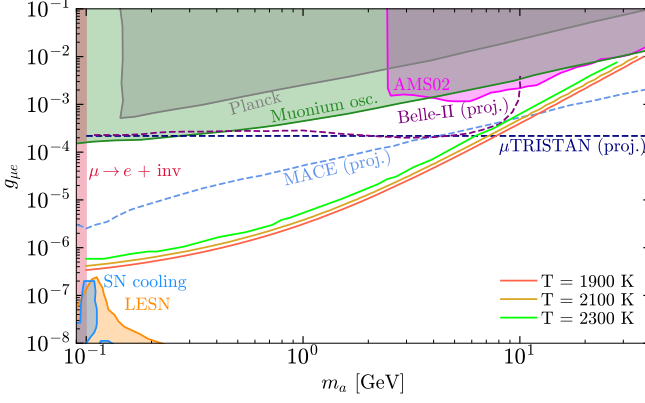


FIG. 3. Current constraints and projected exclusion bounds on the LFV DM model with the ALP mediator and the $m_\chi = 2m_a$ mass hierarchy in the $(m_a, g_{\mu e})$ plane. The green (brown, red) solid lines define the lower boundary of the regions in the parameter space where DM-induced kinetic and annihilation heating is expected to sustain neutron star temperatures above 2300 K (2100 K, 1900 K) even for old NSs.

peratures $T \lesssim 2000$ K. For sufficiently high $g_{\mu e}$, DM-induced heating is expected to prevent NSs from cooling below the temperatures indicated in the plot. The results shown here are obtained for $m_\chi = 2m_a$. For each DM mass, we assume the thermal value of the dark coupling constant g_χ , which guarantees the correct DM relic density for any value of $g_{\mu e}$.

Current bounds on this scenario primarily result from searches for LFV ALPs. Light ALPs with $m_a < m_\mu - m_e$ are strongly constrained by the search for the invisible muon decay $\mu \rightarrow e + \text{inv.}$ [50]. These particles, produced in the two-body muon decay, $\mu \rightarrow ea$, subsequently decay into electrons and neutrinos (e.g., $a \rightarrow e^+e^-\nu_\mu\bar{\nu}_e$) with a sufficiently large lifetime that they mimic invisible energy loss in the detector. For light DM, three-body decays via off-shell ALPs, $\mu \rightarrow e\chi\bar{\chi}$, are also possible. Light ALPs are, therefore, excluded in the $g_{\mu e}$ coupling regime of our interest. For small such couplings, astrophysical bounds derived from supernovae cooling and low-energy supernovae (LESN) explosions extend these constraints up to $m_a \sim 500$ MeV [25, 50, 62–64].

For even heavier ALPs, the upper bound on $g_{\mu e} \lesssim 10^{-3}$ is primarily driven by constraints from the search for spontaneous muonium-antimuonium conversion [72]; cf. also Refs [46, 61]. In the plot, we also present relevant future projected constraints from the MACE experiment [73]. We also show the expected bounds from the search for LFV ALPs in the proposed μ TRISTAN experiment [61] and the projected Belle-II sensitivity obtained with 50 ab^{-1} of integrated luminosity, derived from the search for explicit LFV in the $e^+e^- \rightarrow \mu^\pm\mu^\pm e^\mp e^\mp$ process [47]. As can be seen, future NS bounds can surpass all these experimental projections for ALP masses up to $m_a \sim$ a few GeV and close the gap between them and

supernovae constraints for $m_a \sim m_\mu$.

In the plot, we also present DM ID constraints derived from observations of the Cosmic Microwave Background (CMB) by the Planck collaboration [66] and from positron measurements by AMS-02 [74]. Notably, these limits are based on the suppressed s -wave annihilation mode, $\chi\bar{\chi} \rightarrow e\mu$, which is sensitive to small values of $g_{\mu e}$. We rescale the more stringent existing bounds on DM annihilation into an e^+e^- final state to account for the weaker impact of muons in the final state, cf. also recent analysis in Ref. [75]. As can be seen in the plot, the DM ID limits remain at most comparable to the muonium oscillation bound. A potential future improvement of these bounds by an order of magnitude in the annihilation cross section [76, 77] would help constrain $g_{\mu e}$ by an additional factor of a few.

Instead, future observations of old NSs could provide significantly stronger constraints on this scenario, potentially by three orders of magnitude in $g_{\mu e}$ at sub-GeV masses. Remarkably, the DM-induced NS heating is primarily driven by p -wave secluded annihilations, $\chi\bar{\chi} \rightarrow aa$, with the subsequent ALP decay inside the star, $a \rightarrow \mu e$. These p -wave annihilations are much less suppressed than for DM ID due to two key effects: *i*) boosting of DM particles in the NS gravitational field, and *ii*) flavor blocking of their equilibration with the star's temperature, which enhances the characteristic DM velocity in the NS.

While future observations of cold NSs with temperatures $T \sim \mathcal{O}(10^3 \text{ K})$ would allow for strongly constraining the parameter space of the LFV DM model under study, discovering DM this way requires additional caution. Other NS heating mechanisms have been proposed that would not require DM capture. However, these mechanisms remain speculative and typically rely on additional assumptions about the NS's evolution and spin, cf. Ref. [24] for a review. Therefore, future observations of a population of old NSs with $T \gtrsim 2000$ K could still be indicative of new physics.

In the specific case of LFV DM, these observations will be especially important, as traditional DD and ID searches suffer from kinematical threshold effects and low interaction rates, respectively. If a LFV ALP signal were found in future accelerator facilities, observations of old NSs would allow us to connect this discovery to DM, therefore bridging the gap between particle physics and astrophysics in probing one of the few remaining thermal DM targets.

We have illustrated our findings for a specific ALP mediator with a mass at the GeV scale, which has recently received much attention and can lead to secluded thermal DM targets. We note, however, that the discussed flavor-blocking mechanism remains more broadly applicable to LFV interactions of DM within neutron stars. For bosonic DM particles, it is known that even the existence of old NSs imposes bounds on asymmetric DM

scenarios that predict black hole formation and subsequent stellar collapse [78]. In the presence of flavor blocking, this constraint can be mitigated due to an increased isothermal radius sphere, which is driven by the high DM temperature. For LFV DM species with $m_\chi \ll \text{GeV}$, the relevant radius might extend beyond the star's surface. In this case, efficient p -wave DM annihilations, which are typically strongly suppressed in the outer Galaxy, might lead to additional indirect detection signatures. Future studies should detail this potential LFV-specific impact of DM interactions on neutron stars.

Digital data for this work, including the complete neutron star profile, can be found as ancillary files in the arXiv submission [79].

Acknowledgments: The work of H. D. is supported by the US Department of Energy under Grant Contract DE-SC0012704. J. H. Z. and S. T. are supported by the National Science Centre, Poland (research grant No. 2021/42/E/ST2/00031). ST is also partially supported by Teaming for Excellence grant Astrocent Plus (GA: 101137080) funded by the European Union.

* hooman@bnl.gov

† jaime.hoefkenzink@ncbj.gov.pl

‡ sebastian.trojanowski@ncbj.gov.pl

- [1] L. Roszkowski, E. M. Sessolo, and S. Trojanowski, *Rept. Prog. Phys.* **81**, 066201 (2018), arXiv:1707.06277 [hep-ph].
- [2] J. Billard *et al.*, *Rept. Prog. Phys.* **85**, 056201 (2022), arXiv:2104.07634 [hep-ex].
- [3] A. Boveia *et al.*, (2022), arXiv:2210.01770 [hep-ph].
- [4] R. Alves Batista *et al.*, (2021), arXiv:2110.10074 [astro-ph.HE].
- [5] C. Kouvaris, *Phys. Rev. D* **77**, 023006 (2008), arXiv:0708.2362 [astro-ph].
- [6] G. Bertone and M. Fairbairn, *Phys. Rev. D* **77**, 043515 (2008), arXiv:0709.1485 [astro-ph].
- [7] C. Kouvaris and P. Tinyakov, *Phys. Rev. D* **82**, 063531 (2010), arXiv:1004.0586 [astro-ph.GA].
- [8] A. de Lavallaz and M. Fairbairn, *Phys. Rev. D* **81**, 123521 (2010), arXiv:1004.0629 [astro-ph.GA].
- [9] B. Bertoni, A. E. Nelson, and S. Reddy, *Phys. Rev. D* **88**, 123505 (2013), arXiv:1309.1721 [hep-ph].
- [10] M. Baryakhtar, J. Bramante, S. W. Li, T. Linden, and N. Raj, *Phys. Rev. Lett.* **119**, 131801 (2017), arXiv:1704.01577 [hep-ph].
- [11] J. Bramante, A. Delgado, and A. Martin, *Phys. Rev. D* **96**, 063002 (2017), arXiv:1703.04043 [hep-ph].
- [12] N. Raj, P. Tanedo, and H.-B. Yu, *Phys. Rev. D* **97**, 043006 (2018), arXiv:1707.09442 [hep-ph].
- [13] N. F. Bell, G. Busoni, and S. Robles, *JCAP* **09**, 018 (2018), arXiv:1807.02840 [hep-ph].
- [14] J. F. Acevedo, J. Bramante, R. K. Leane, and N. Raj, *JCAP* **03**, 038 (2020), arXiv:1911.06334 [hep-ph].
- [15] N. F. Bell, G. Busoni, S. Robles, and M. Virgato, *JCAP* **09**, 028 (2020), arXiv:2004.14888 [hep-ph].
- [16] N. F. Bell, G. Busoni, T. F. Motta, S. Robles, A. W. Thomas, and M. Virgato, *Phys. Rev. Lett.* **127**, 111803 (2021), arXiv:2012.08918 [hep-ph].
- [17] R. Garani, A. Gupta, and N. Raj, *Phys. Rev. D* **103**, 043019 (2021), arXiv:2009.10728 [hep-ph].
- [18] B. Dasgupta, A. Gupta, and A. Ray, *JCAP* **10**, 023 (2020), arXiv:2006.10773 [hep-ph].
- [19] F. Anzuini, N. F. Bell, G. Busoni, T. F. Motta, S. Robles, A. W. Thomas, and M. Virgato, *JCAP* **11**, 056 (2021), [Erratum: *JCAP* **04**, E02 (2024)], arXiv:2108.02525 [hep-ph].
- [20] W. DeRocco, M. Galanis, and R. Lasenby, *JCAP* **05**, 015 (2022), arXiv:2201.05167 [hep-ph].
- [21] J. Coffey, D. McKeen, D. E. Morrissey, and N. Raj, *Phys. Rev. D* **106**, 115019 (2022), arXiv:2207.02221 [hep-ph].
- [22] T. T. Q. Nguyen and T. M. P. Tait, *Phys. Rev. D* **107**, 115016 (2023), arXiv:2212.12547 [hep-ph].
- [23] N. F. Bell, G. Busoni, S. Robles, and M. Virgato, *JCAP* **04**, 006 (2024), arXiv:2312.11892 [hep-ph].
- [24] J. Bramante and N. Raj, *Phys. Rept.* **1052**, 1 (2024), arXiv:2307.14435 [hep-ph].
- [25] H.-Y. Zhang, R. Hagimoto, and A. J. Long, *Phys. Rev. D* **109**, 103005 (2024), arXiv:2309.03889 [hep-ph].
- [26] L. Su, L. Wu, and M. Yang, *Phys. Rev. D* **110**, 055014 (2024), arXiv:2408.03759 [hep-ph].
- [27] Y. Ema, R. McGehee, M. Pospelov, and A. Ray, *Phys. Rev. D* **111**, 023005 (2025), arXiv:2405.18472 [hep-ph].
- [28] I. Goldman and S. Nussinov, *Phys. Rev. D* **40**, 3221 (1989).
- [29] S. D. McDermott, H.-B. Yu, and K. M. Zurek, *Phys. Rev. D* **85**, 023519 (2012), arXiv:1103.5472 [hep-ph].
- [30] J. Bramante and T. Linden, *Phys. Rev. Lett.* **113**, 191301 (2014), arXiv:1405.1031 [astro-ph.HE].
- [31] R. Garani, Y. Genolini, and T. Hambye, *JCAP* **05**, 035 (2019), arXiv:1812.08773 [hep-ph].
- [32] N. F. Bell, G. Busoni, and S. Robles, *JCAP* **06**, 054 (2019), arXiv:1904.09803 [hep-ph].
- [33] A. Joglekar, N. Raj, P. Tanedo, and H.-B. Yu, *Phys. Lett. B* **809**, 135767 (2020), arXiv:1911.13293 [hep-ph].
- [34] A. Joglekar, N. Raj, P. Tanedo, and H.-B. Yu, *Phys. Rev. D* **102**, 123002 (2020), arXiv:2004.09539 [hep-ph].
- [35] N. F. Bell, G. Busoni, S. Robles, and M. Virgato, *JCAP* **03**, 086 (2021), arXiv:2010.13257 [hep-ph].
- [36] P. Haensel, A. Y. Potekhin, and D. G. Yakovlev, *Neutron stars 1: Equation of state and structure*, Vol. 326 (Springer, New York, USA, 2007).
- [37] R. Garani and J. Heeck, *Phys. Rev. D* **100**, 035039 (2019), arXiv:1906.10145 [hep-ph].
- [38] L. Di Luzio, M. Giannotti, E. Nardi, and L. Visinelli, *Phys. Rept.* **870**, 1 (2020), arXiv:2003.01100 [hep-ph].
- [39] K. Choi, S. H. Im, and C. Sub Shin, *Ann. Rev. Nucl. Part. Sci.* **71**, 225 (2021), arXiv:2012.05029 [hep-ph].
- [40] M. Bauer, M. Neubert, S. Renner, M. Schnubel, and A. Thamm, *JHEP* **04**, 063 (2021), arXiv:2012.12272 [hep-ph].
- [41] A. Davidson and K. C. Wali, *Phys. Rev. Lett.* **48**, 11 (1982).
- [42] F. Wilczek, *Phys. Rev. Lett.* **49**, 1549 (1982).
- [43] M. Bauer, T. Schell, and T. Plehn, *Phys. Rev. D* **94**, 056003 (2016), arXiv:1603.06950 [hep-ph].
- [44] K. Choi, S. H. Im, C. B. Park, and S. Yun, *JHEP* **11**, 070 (2017), arXiv:1708.00021 [hep-ph].
- [45] B. Batell, H. Davoudiasl, R. Marcarelli, E. T. Neil,

- and S. Trojanowski, *Phys. Rev. D* **110**, 075039 (2024), [arXiv:2407.15942 \[hep-ph\]](#).
- [46] P. S. B. Dev, R. N. Mohapatra, and Y. Zhang, *Phys. Rev. Lett.* **120**, 221804 (2018), [arXiv:1711.08430 \[hep-ph\]](#).
- [47] M. Endo, S. Iguro, and T. Kitahara, *JHEP* **06**, 040 (2020), [arXiv:2002.05948 \[hep-ph\]](#).
- [48] M. Bauer, M. Neubert, S. Renner, M. Schnubel, and A. Thamm, *Phys. Rev. Lett.* **124**, 211803 (2020), [arXiv:1908.00008 \[hep-ph\]](#).
- [49] C. Cornella, P. Paradisi, and O. Sumensari, *JHEP* **01**, 158 (2020), [arXiv:1911.06279 \[hep-ph\]](#).
- [50] L. Calibbi, D. Redigolo, R. Ziegler, and J. Zupan, *JHEP* **09**, 173 (2021), [arXiv:2006.04795 \[hep-ph\]](#).
- [51] S. N. Gninenko, M. M. Kirsanov, N. V. Krasnikov, and V. A. Matveev, *Mod. Phys. Lett. A* **17**, 1407 (2002), [arXiv:hep-ph/0106302](#).
- [52] S. Gninenko, S. Kovalenko, S. Kuleshov, V. E. Lyubovitskij, and A. S. Zhevlakov, *Phys. Rev. D* **98**, 015007 (2018), [arXiv:1804.05550 \[hep-ph\]](#).
- [53] H. Davoudiasl, R. Marcarelli, N. Miesch, and E. T. Neil, *Phys. Rev. D* **104**, 055022 (2021), [arXiv:2105.05866 \[hep-ph\]](#).
- [54] K. Cheung, A. Soffer, Z. S. Wang, and Y.-H. Wu, *JHEP* **11**, 218 (2021), [arXiv:2108.11094 \[hep-ph\]](#).
- [55] M. Bauer, M. Neubert, S. Renner, M. Schnubel, and A. Thamm, *JHEP* **09**, 056 (2022), [arXiv:2110.10698 \[hep-ph\]](#).
- [56] H. Davoudiasl, R. Marcarelli, and E. T. Neil, *JHEP* **02**, 071 (2023), [arXiv:2112.04513 \[hep-ph\]](#).
- [57] G. Haghighat and M. Mohammadi Najafabadi, *Nucl. Phys. B* **980**, 115827 (2022), [arXiv:2106.00505 \[hep-ph\]](#).
- [58] Y. Ema, Z. Liu, K.-F. Lyu, and M. Pospelov, *JHEP* **02**, 135 (2023), [arXiv:2211.00664 \[hep-ph\]](#).
- [59] B. Radics, L. Molina-Bueno, L. Fields., H. Sieber, and P. Crivelli, *Eur. Phys. J. C* **83**, 775 (2023), [arXiv:2306.07405 \[hep-ex\]](#).
- [60] H. Davoudiasl, R. Marcarelli, and E. T. Neil, *Phys. Rev. D* **109**, 115013 (2024), [arXiv:2402.17821 \[hep-ph\]](#).
- [61] L. Calibbi, T. Li, L. Mukherjee, and Y. Yang, *Phys. Rev. D* **110**, 115009 (2024), [arXiv:2406.13234 \[hep-ph\]](#).
- [62] Y. Li and Z. Liu, (2025), [arXiv:2501.12075 \[hep-ph\]](#).
- [63] Z.-M. Huang and Z. Liu, (2025), [arXiv:2506.16922 \[hep-ph\]](#).
- [64] Z.-M. Huang, C. Li, and Z. Liu, (2025), [arXiv:2510.22523 \[hep-ph\]](#).
- [65] G. Armando, P. Panci, J. Weiss, and R. Ziegler, *Phys. Rev. D* **109**, 055029 (2024), [arXiv:2310.05827 \[hep-ph\]](#).
- [66] N. Aghanim *et al.* (Planck), *Astron. Astrophys.* **641**, A6 (2020), [Erratum: *Astron. Astrophys.* 652, C4 (2021)], [arXiv:1807.06209 \[astro-ph.CO\]](#).
- [67] Y. Xu, S. Goriely, A. Jorissen, G. Chen, and M. Arnould, *Astron. Astrophys.* **549**, A106 (2013), [arXiv:1212.0628 \[nucl-th\]](#).
- [68] S. Goriely, N. Chamel, and J. M. Pearson, *Phys. Rev. C* **88**, 061302 (2013).
- [69] L. Perot, N. Chamel, and A. Sourie, *Phys. Rev. C* **100**, 035801 (2019), [arXiv:1910.13202 \[nucl-th\]](#).
- [70] S. Chatterjee, R. Garani, R. K. Jain, B. Kanodia, M. S. N. Kumar, and S. K. Vempati, *Phys. Rev. D* **108**, L021301 (2023), [arXiv:2205.05048 \[astro-ph.HE\]](#).
- [71] J. F. Acevedo, J. Bramante, Q. Liu, and N. Tyagi, (2024), [arXiv:2404.10039 \[hep-ph\]](#).
- [72] L. Willmann *et al.*, *Phys. Rev. Lett.* **82**, 49 (1999), [arXiv:hep-ex/9807011](#).
- [73] A.-Y. Bai *et al.*, in *Snowmass 2021* (2022) [arXiv:2203.11406 \[hep-ph\]](#).
- [74] I. John and T. Linden, *JCAP* **12**, 007 (2021), [arXiv:2107.10261 \[astro-ph.HE\]](#).
- [75] J.-H. Liang, Y. Liao, and X.-D. Ma, (2025), [arXiv:2508.05121 \[hep-ph\]](#).
- [76] J. Cooley *et al.*, (2022), [arXiv:2209.07426 \[hep-ph\]](#).
- [77] Y.-N. Wang, X.-C. Duan, T.-P. Tang, Z. Wang, and Y.-L. S. Tsai, *JCAP* **08**, 059 (2025), [arXiv:2502.18263 \[hep-ph\]](#).
- [78] K. M. Zurek, *Phys. Rept.* **537**, 91 (2014), [arXiv:1308.0338 \[hep-ph\]](#).
- [79] H. Davoudiasl, J. Hoefken Zink, and S. Trojanowski, *GitHub repository – main plots data and star profile* (2025).
- [80] J. M. Pearson, N. Chamel, A. Y. Potekhin, A. F. Fantina, C. Ducoin, A. K. Dutta, and S. Goriely, *Mon. Not. Roy. Astron. Soc.* **481**, 2994 (2018), [Erratum: *Mon. Not. Roy. Astron. Soc.* 486, 768 (2019)], [arXiv:1903.04981 \[astro-ph.HE\]](#).
- [81] A. Akmal, V. R. Pandharipande, and D. G. Ravenhall, *Phys. Rev. C* **58**, 1804 (1998), [arXiv:nucl-th/9804027](#).
- [82] J. Rikowska-Stone, P. A. M. Guichon, H. H. Matevosyan, and A. W. Thomas, *Nucl. Phys. A* **792**, 341 (2007), [arXiv:nucl-th/0611030](#).
- [83] S. Goriely, N. Chamel, and J. M. Pearson, *Phys. Rev. C* **82**, 035804 (2010), [arXiv:1009.3840 \[nucl-th\]](#).
- [84] J. M. Pearson, S. Goriely, and N. Chamel, *Phys. Rev. C* **83**, 065810 (2011).
- [85] J. M. Pearson, N. Chamel, S. Goriely, and C. Ducoin, *Phys. Rev. C* **85**, 065803 (2012), [arXiv:1206.0205 \[nucl-th\]](#).
- [86] S. Goriely, N. Chamel, and J. M. Pearson, *Phys. Rev. C* **88**, 024308 (2013).
- [87] A. Y. Potekhin, A. F. Fantina, N. Chamel, J. M. Pearson, and S. Goriely, *Astron. Astrophys.* **560**, A48 (2013), [arXiv:1310.0049 \[astro-ph.SR\]](#).
- [88] T. Kojo, P. D. Powell, Y. Song, and G. Baym, *Phys. Rev. D* **91**, 045003 (2015), [arXiv:1412.1108 \[hep-ph\]](#).
- [89] G. Baym, T. Hatsuda, T. Kojo, P. D. Powell, Y. Song, and T. Takatsuka, *Rept. Prog. Phys.* **81**, 056902 (2018), [arXiv:1707.04966 \[astro-ph.HE\]](#).
- [90] E. Annala, T. Gorda, A. Kurkela, J. Nättilä, and A. Vuorinen, *Mem. Soc. Ast. It.* **90**, 81 (2019), [arXiv:1904.01354 \[astro-ph.HE\]](#).
- [91] W.-C. Chen and J. Piekarewicz, *Phys. Rev. C* **90**, 044305 (2014), [arXiv:1408.4159 \[nucl-th\]](#).
- [92] C. Huang, G. Raaijmakers, A. L. Watts, L. Tolos, and C. Providência, *Mon. Not. Roy. Astron. Soc.* **529**, 4650 (2024), [arXiv:2303.17518 \[astro-ph.HE\]](#).
- [93] R. C. Tolman, *Phys. Rev.* **55**, 364 (1939).
- [94] J. R. Oppenheimer and G. M. Volkoff, *Phys. Rev.* **55**, 374 (1939).
- [95] C. Huang and X.-P. Zheng, (2024), [arXiv:2409.18432 \[astro-ph.HE\]](#).
- [96] C. Huang *et al.*, (2024), [arXiv:2411.14615 \[astro-ph.HE\]](#).
- [97] C. Huang, L. Tolos, C. Providência, and A. Watts, *Mon. Not. Roy. Astron. Soc.* **536**, 3262 (2025), [arXiv:2410.14572 \[astro-ph.HE\]](#).

ALP LFV and neutron stars

(Supplemental Material)

Hooman Davoudiasl¹, Jaime Hoefken Zink², Sebastian Trojanowski^{2,3}

¹ *High Energy Theory Group, Physics Department, Brookhaven National Laboratory, Upton, NY 11973, USA*

² *National Centre for Nuclear Research, Pasteura 7, Warsaw, PL-02-093, Poland*

³ *Astrocent, Nicolaus Copernicus Astronomical Center Polish Academy of Sciences, ul. Rektorska 4, 00-614, Warsaw, Poland*

CAPTURE RATE OF DARK MATTER

Neutron stars

Neutron stars (NSs) are extremely dense stellar remnants. As schematically illustrated in fig. 1, the NS crust typically extends to a depth of up to a few hundred meters from its surface. Below this, one finds the NS core with a high density, $\rho \gtrsim 1.4 \times 10^{14} \text{ g cm}^{-3}$ [80]. In our analysis, we consider the standard case of $npe\mu$ matter, meaning we assume NSs are primarily composed of neutrons, protons, electrons, and muons, and we neglect the presence of hyperons. Many approaches exist to model the Equation of State (EoS) of an NS [80–90]. Two of the most important are the unified EoS for cold, non-accreting matter, based on Brussels-Montreal functionals [80, 83–87], and the relativistic mean-field (RMF) approach [91, 92]. We focus on old and cold stars and, for illustration, we employ the specific BSk-25 EoS (Brussels-Montreal). We use this EoS as an input to solve the structure equations for static matter, known as the Tolman-Oppenheimer-Volkoff (TOV) equations [93, 94].

In order to produce the NS profiles, we have used a version of the software *CompactObject* [92, 95–97], modified by us to print the radius, mass, pressure and energy density in each step of the numerical solution of the TOV equations. We also solve the equations for a range of energy densities at $r = 0$, so that we can interpolate the density needed to produce a precise mass NS we want to generate. After generating the first elements of the profile, we use the EoS to obtain the neutron, proton and lepton chemical potentials, and the baryon number density by interpolating the expected values given a fixed energy density. For the number densities, we obtain the leptonic ones by considering a zero-temperature, free, relativistic Fermi gas:

$$n_l = \frac{(\mu_l^2 - m_l^2)^{3/2}}{3\pi^2} \times \Theta(\mu_l - m_l), \quad (11)$$

where μ_l and m_l are the lepton chemical potential and masses respectively. This relation is valid for low temperatures as in our case. The number density of the protons is obtained by assuming charge neutrality: $n_p = n_e + n_\mu$. For the neutrons we use: $n_n = n_b - n_p$, where n_b is the baryon number density. Finally, we get the elements of the metric by solving the following:

$$\begin{aligned} |g_{tt}| &= \left(1 - \frac{2GM_{\text{NS}}}{c^2 r}\right) \times \exp\left(-2 \int_0^p \frac{dp'}{p' + e(p')}\right), \\ |g_{rr}| &= \left(1 - \frac{2Gm(r)}{c^2 r}\right)^{-1}, \end{aligned} \quad (12)$$

where $e(p)$ is the energy density as a function of pressure and the results obtained depend on the position (r) and the pressure at that point (for g_{tt}) and on the position and the mass inside a sphere of radius r ($m(r)$). All this data is put into tables so that any needed quantity can be interpolated for a given r .

Capture rate expression

Capture of DM particles takes place as they are attracted by the gravitational force of the star and when they interact with its matter, so that the outgoing DM fermion cannot escape. In our case, since the interactions are with

degenerate leptons and because we are considering very cold stars, if an interaction takes place, then the DM particle is automatically captured. This is because the target lepton has an energy below the leptonic chemical potential, μ_l , while the outgoing above μ_l . Therefore, the DM fermion will lose energy and, due to starting its motion roughly at rest, $v_\infty \sim 0$, then any energy loss will imply being gravitationally captured.

There are two possible interactions at tree level that can lead to capture DM: $\chi + e \rightarrow \chi + \mu$ and $\chi + \mu \rightarrow \chi + e$. We will work on the kinematics using the following notation: any 4-vector will just be represented by a letter with a subscript number (P_i), where $i = 1$ will denote ingoing and $i = 2$ outgoing. k will be used for the DM particles, while p for the leptons. The energy and 3-momentum magnitude of a particle with 4-momentum P_i will be E_{P_i} and p_{P_i} respectively.

The mean amplitude squared of any of the mentioned processes is:

$$\begin{aligned} \langle |\mathcal{M}|^2 \rangle &= \frac{g_\chi^2 g_{\mu e}^2}{(t - m_a^2)^2} t \\ &\times (t - m_\mu^2 + 2m_\mu m_e \cos(2\phi) - m_e^2) . \end{aligned} \quad (13)$$

where $t \equiv (k_1 - k_2)^2$ is the Mandelstam variable. The relevant differential cross section reads:

$$\frac{d\sigma}{d\cos\theta_{\text{cm}} d\alpha \rightarrow \beta} = \frac{\langle |\mathcal{M}|^2 \rangle}{32\pi s} \frac{g_s(m_\beta)}{g_s(m_\alpha)} , \quad (14)$$

where θ_{cm} is the angle between the incoming and outgoing DM particles in the CM frame, the target and outgoing leptons are ℓ_α and ℓ_β respectively, $g_s(m) \equiv \sqrt{s^2 - 2(m_\chi^2 + m^2)s + (m_\chi^2 - m^2)^2}$ and $s \equiv (k_1 + p_1)^2$ is the Mandelstam variable.

Since we have two channels, the expression for the interaction rate takes a more complicated form than the one in Ref. [15]: $\Omega^- \equiv \Omega_{\mu \rightarrow e}^- + \Omega_{e \rightarrow \mu}^-$, such that

$$\Omega_{\alpha \rightarrow \beta}^- = \frac{\zeta}{32\pi^3 m_\chi} \sqrt{\frac{g_{tt}}{1 - g_{tt}}} \int_{m_\alpha}^{\mu_l} dE_{p_1} E_{p_1} \int_{s_{\min}}^{s_{\max}} \frac{s ds}{g_s(m_\alpha) \beta_s(m_\alpha)} \int_{t_{\min}}^{t_{\max}} dt \langle |\mathcal{M}| \rangle \Theta(E_{p_2} - \mu_l) , \quad (15)$$

where $\zeta \equiv n_\alpha/n_{\text{free}}$ is a correction to the target number density as was computed by [31], μ_l is the leptonic chemical potential, $t \equiv (k_1 - k_2)^2$ is the Mandelstam variable, $\beta_s(m) \equiv s^2 - (m_\chi^2 - m^2)^2$. The Mandelstam variables limiting values are:

$$s_{\min,1} \leq s \leq s_{\max} \wedge (m_\chi + \max(m_\alpha, m_\beta))^2 \leq s , \quad (16)$$

such that $s_{\min,1/\max} \equiv m_\chi^2 + m_\alpha^2 + 2E_{k_1} E_{p_1} \mp 2p_{k_1} p_{p_1}$. s_{\min} is the maximum value of $s_{\min,1}$ and $(m_\chi + \max(m_\alpha, m_\beta))^2$. For t we have:

$$t_{\min/\max} = - \frac{s^2 - A_t s + B_t \pm \gamma_s(m_\alpha) \gamma_s(m_\beta)}{2s} , \quad (17)$$

where $A_t \equiv (m_\alpha^2 + m_\beta^2 + 2m_\chi^2)$ and $B_t \equiv (m_\alpha^2 - m_\chi^2)(m_\beta^2 - m_\chi^2)$. The energy of the outgoing target, E_{p_2} , is a long expression that depends on E_{k_1} , E_{p_1} , s , t and the masses. This approach considers one scattering for capture. We have also considered multiple scattering [15], though they do not alter our results for the masses taken into account.

Optical factor

After defining the saturation limit as the minimum value of the cross section for which all DM particles get captured and the geometric limit as the minimum limit for which all the DM particles get captured within a thin shell close to the surface of the star, we can study the optical factor as a function of the radial position in the star for those limiting situation. The optical factor represents the amount of flux that remains along a trajectory for a point

at r , given that the motion was from $r' = R_{\text{NS}}$ to $r' = r$. To compute the relative quantity of flux that is absorbed for some radial position r , which is the only parameter needed due to spherical symmetry, we need to take into account the definition of the interaction rate, $\Omega^-(r)$, which is the probability rate of being captured as seen from far from the NS. Therefore, as seen locally, this quantity would be $\Omega^-(r)/\sqrt{g_{tt}(r)}$. In the following, we will leave the radial dependency implicit, for simplicity.

Taking the definition of $\Omega^-/\sqrt{g_{tt}}$, the equation for the evolution of the number of particles going through a particular geodesic at a position r is:

$$\frac{dN}{dt^{\text{loc}}} = -\frac{\Omega^-}{\sqrt{g_{tt}}} N, \quad (18)$$

whose solution is:

$$\frac{N}{N_0} = e^{-\int dt^{\text{loc}} \frac{\Omega^-}{\sqrt{g_{tt}}}} = \eta, \quad (19)$$

where η is the optical factor and represents the relative quantity of flux that reaches the position r through a particular geodesic, and t^{loc} refers to local proper time in an orthonormal basis at r .

To compute kinematical quantities for a particular geodesic, we look at the equations of motion. These geodesic equations are written in terms of conserved quantities in the coordinate basis: $\mathcal{E} \equiv \frac{E_\chi^\infty}{m_\chi} = 1$ and $\mathcal{L} = \frac{J}{m_\chi}$. We replace these quantities directly and consider motion on the equatorial plane, $\theta = \pi/2$:

$$\begin{aligned} \frac{dt}{d\tau} = u^t &= \frac{1}{g_{tt}}, \\ \frac{dr}{d\tau} = u^r &= \pm \sqrt{\frac{1}{g_{tt}g_{rr}} - \frac{1}{g_{rr}} \left(1 + \frac{J^2}{m_\chi^2 r^2}\right)}, \\ \frac{d\phi}{d\tau} = u^\phi &= \frac{J}{m_\chi r^2}, \\ \frac{d\theta}{d\tau} = u^\theta &= 0. \end{aligned} \quad (20)$$

The sign of u^r depends on whether the trajectory has already passed the minimum radius, $r = r_{\text{min}}$. The coordinate time increment satisfies $dt^{\text{loc}} = \sqrt{g_{tt}} dt$, so that,

$$\eta = e^{-\int dt \Omega^-}. \quad (21)$$

Since absorption depends only on r , we convert dt to dr :

$$\begin{aligned} \int dt \Omega^- &= \int dr' \frac{dt}{dr'} \Omega^- = \int dr' \frac{dt/d\tau}{dr'/d\tau} \Omega^- = \int dr' \frac{1/g_{tt}}{\sqrt{\frac{1}{g_{tt}g_{rr}} - \frac{1}{g_{rr}} \left(1 + \frac{J^2}{m_\chi^2 r'^2}\right)}} \Omega^-, \\ &= \int dr' \sqrt{\frac{g_{rr}}{g_{tt}(1-g_{tt})}} \frac{1}{\sqrt{1 - \frac{J^2}{\frac{1-g_{tt}}{g_{tt}} m_\chi^2 r'^2}}} \Omega^-, \end{aligned} \quad (22)$$

where we use a prime, r' , not to confuse the radius along the geodesic with the point at which we are computing η and all the metric elements are evaluated at r' . This expression simplifies using the maximum angular momentum for which the radial motion is allowed:

$$\frac{1}{g_{tt}g_{rr}} - \frac{1}{g_{rr}} \left(1 + \frac{J^2}{m_\chi^2 r^2}\right) \geq 0 \quad \Rightarrow \quad J_{\text{max}}^2 = \frac{1-g_{tt}}{g_{tt}} m_\chi^2 r^2, \quad (23)$$

so that:

$$\int dt \Omega^- = \int dr' \sqrt{\frac{g_{rr}}{g_{tt}(1-g_{tt})}} \frac{1}{\sqrt{1 - \frac{J^2}{J_{\text{max}}^2(r')}}} \Omega^-, \quad (24)$$

where we have found an extra factor, $\sqrt{g_{rr}/g_{tt}}$, with respect to previous treatments. We parameterize J as a fraction y of its maximum at r :

$$J \equiv y J_{\max}(r),$$

where $y = \sin \theta$ in classical terms, where θ is the angle between the geodesic and \vec{r} . Then:

$$\int dt \Omega^- = \int dr' \frac{\sqrt{g_{rr}}}{1 - g_{tt}} \frac{1}{\sqrt{1 - y^2 \frac{J_{\max}^2(r)}{J_{\max}^2(r')}}} \Omega^- . \quad (25)$$

For fixed J (or y), there are two trajectories: one from the surface and just decreasing in r' down to r , and another that goes to r_{\min} and returns to r . These define two path integrals:

$$\begin{aligned} \tau_{\chi}^-(r, y) &= \int_r^{R_{\text{NS}}} dr' \sqrt{\frac{g_{rr}}{g_{tt}(1 - g_{tt})}} \frac{1}{\sqrt{1 - y^2 \frac{J_{\max}^2(r)}{J_{\max}^2(r')}}} \Omega^- , \\ \tau_{\chi}^+(r, y) &= \tau_{\chi}^-(r, y) + 2 \int_{r_{\min}}^r dr' \sqrt{\frac{g_{rr}}{g_{tt}(1 - g_{tt})}} \frac{1}{\sqrt{1 - y^2 \frac{J_{\max}^2(r)}{J_{\max}^2(r')}}} \Omega^- . \end{aligned} \quad (26)$$

To obtain the total suppression factor, we average over the distribution of angular momenta:

$$\eta = \frac{1}{2} \int f(y) dy \left[e^{-\tau_{\chi}^-(r, y)} + e^{-\tau_{\chi}^+(r, y)} \right] . \quad (27)$$

Since $y = \sin \theta$ and θ is distributed as $p_{\theta}(\theta) d\theta = \sin \theta d\theta$, and using $\theta = \sin^{-1} y$ with $d\theta/dy = 1/\sqrt{1 - y^2}$, we get:

$$p_{\theta}(\theta) d\theta = \frac{y}{\sqrt{1 - y^2}} dy . \quad (28)$$

Therefore, the final expression for η is:

$$\eta = \frac{1}{2} \int \frac{y}{\sqrt{1 - y^2}} dy \left[e^{-\tau_{\chi}^-(r, y)} + e^{-\tau_{\chi}^+(r, y)} \right] . \quad (29)$$

Saturation and geometric limit

We want to redefine and distinguish two concepts that were usually used interchangeably, but whose distinction is important to analyze the effects of capture rate: saturation and geometric limit.

We define the saturation limit as the lower limit of the cross section (or of a coupling), for which the star starts to be able to capture all the DM particles in it. In terms of the optical factor, it would be the minimum value of the cross section (or couplings) for which $\eta(0) = 0$.

We will consider the geometric limit to be the lower limit of the cross section (or couplings) for which everything gets captured on a thin shell of negligible thickness, usually close to the NS's surface. In this case, the optical factor takes the form of a step function: $\eta(r) = \Theta(r - R_{\text{eff}})$, where R_{eff} is the position of the shell. In general, this shell is the NS surface. However, in our case, since the outer part of the star just has electrons and since the upscattering to muons is just permitted for some limiting lower value of the chemical potential, so that the electrons have enough energy to upscatter to a muon, there is an effective radius that we have found to be greater than the muon radius (the NS region with muons), R_{μ} , but less than the radius of the whole star: $R_{\mu} \leq R_{\text{eff}} \leq R_{\text{NS}}$.

For all the parameters space between these two situations, everything is captured and the capture rate in this regime is [13]:

$$C_{\text{NS}} = \frac{\pi R_{\text{NS}}^2 (1 - B(R_{\text{NS}}))}{v_{\text{NS}} B(R_{\text{NS}})} \frac{\rho_{\chi}}{m_{\chi}} \text{Erf} \left(\sqrt{\frac{3}{2}} \frac{v_{\text{NS}}}{v_d} \right) , \quad (30)$$

where $B(r) \equiv 1 - 2GM_{\text{NS}}/c^2 r$. As it will be seen in the results, R_{NS} should really be R_{eff} , the effective radius where interactions take place when we go to the saturation limit. However, this radius is very close to the radius and the difference with respect to the whole star is just negligible.

KINETIC ENERGY DEPOSITION

Because of the subtleties of General Relativity and the non-conservation of local energies, it is important to compute the deposition from the first interaction until the DM loses almost all its kinetic energy. The injection of energy converges to a uniform value when the DM loses almost all of its kinetic energy independently of the number of interactions N . We will not make any assumptions about neither where the interactions take place nor how many there are. We will just suppose the interactions end up at the center of the star, such that their sequence is at arbitrary radial distances (r_i , where $0 \leq i \leq N$) from the center of the star. This sequence goes from the first point where it interacts to the center of the star, where it finishes its journey. We will measure all the energies as seen from the surface. We will not assume the particle has a radial trajectory.

After the DM particle has its n th interaction, it loses a fraction p_n ($0 \leq p_n \leq 1$) of its kinetic energy and gains energy before interacting again from its gravitational pull to the center of the star. To compute the energy gained just by the interaction with the classical gravitational field, we need to consider the invariant quantity: $\mathcal{E} \equiv |g_{\mu\nu} p^\mu \xi^\nu|$, where ξ^ν is the Killing vector equal to $(1, 0, 0, 0)$. If every element of the metric is represented as a positive quantity, the metric around a NS has the form:

$$ds^2 = -g_{tt} dt^2 + g_{rr} dr^2 + r^2 d\Omega^2. \quad (31)$$

Let us consider the invariance of \mathcal{E} along two different points in the trajectory of a free-falling DM particle: at $r = r_a$ and $r = r_b$. In that case, we have: $\mathcal{E} = g_{tt}^{(a)} E_a = g_{tt}^{(b)} E_b$. We need the vierbein $e_t^{\hat{t}} \equiv \sqrt{g_{tt}}$ in order to relate these quantities with the local energy [denoted by superscript (0)] that is involved in the local interactions we are taking into account:

$$E_i^{(0)} = \sqrt{g_{tt}^{(i)}} E_i, \quad (32)$$

where $g_{tt}^{(i)}$ is the metric tt element evaluated at r_i . With these two equalities, we can finally relate the two local energies:

$$\sqrt{g_{tt}^{(a)}} E_a^{(0)} = \sqrt{g_{tt}^{(b)}} E_b^{(0)}. \quad (33)$$

Let us call $E_k^{(N)}$ the kinetic energy deposited after $N + 1$ interactions (from $n = 0$ to $n = N$) and E_N the remaining energy of the particle after those interactions, both as seen from the surface of the NS. We could follow an iterative process as depicted as follows. We first compute the total energy at the place of interaction, E_n^{tot} , when the n th interaction takes place at the position r_n . For $n = 0$, it is given by the boost of the mass, γ_{r_0} , where r_0 is the position of the first interaction. With this energy we can compute the deposited kinetic energy, as seen from the surface, which is $K_n^{\text{in}} = \xi_{r_n} p_n (E_n^{\text{tot}} - m_\chi)$. The outgoing energy, in the reference frame of the n th interaction is $K_n^{\text{out}} = (1 - p_n) (E_n^{\text{tot}} - m_\chi)$. With these two quantities we can compute the next total energy, as $E_{n+1}^{\text{tot}} = \frac{\gamma_{r_{n+1}}}{\gamma_{r_n}} (K_n^{\text{out}} + m_\chi)$. We do this process and collect all the energy deposited into the star, which takes the form:

$$E_k^{(N)} = \gamma_s m_\chi \sum_{n=0}^N p_n \left(1 - \frac{1}{\gamma_{r_n}}\right) \prod_{i=n+1}^{N+1} (1 - p_i), \quad (34)$$

such that $p_{N+1} \equiv 0$ because we consider N to be the last possible interaction before flavor blocking and s stands for “surface.” By computing the final energy left, we can see that it is:

$$E_N = \gamma_s m_\chi - E_k^{(N)}. \quad (35)$$

However, we claim that the DM particle has lost almost all of its energy and to be located close to the center of the star. Therefore, we expect this remaining energy to be $E_N = \xi_0 m_\chi$, where 0 stands for $r = 0$, the center of the NS. So we can compute the total deposited energy as:

$$E_k^{(N)} = (\gamma_s - \xi_0) m_\chi. \quad (36)$$

If we also consider annihilations at the center of the star and assuming that we have reached the equilibrium time, where the number of DM particles annihilating equals the number of the ones captured, then we have to add E_N and the expression modifies to:

$$E_k^{(N)} = \gamma_s m_\chi, \quad (37)$$

which is the total energy of the particle as it goes through the surface of the star. This quantity differs from the one in [23], where the boost is considered at the center of the star and which may overestimate the deposited energy.

This approach establishes the energy used to compute the heating of the NS at the surface. The energy deposited by each particle in its first interaction as seen from the surface, i.e. $E_k \equiv \xi_r q_0 = \xi_r (E_{k_1} - E_{k_2})$, would underestimate the heating. This energy has two main components, $q_0 = E_{\text{Auger}} + \Delta E$: the Auger energy and the energy difference above the Fermi sea. The outgoing lepton must have an energy above the Fermi sea, $E_{p_2} > \mu_l$, due to Pauli blocking. The space occupied by the target lepton is rapidly filled by nearby leptons below the Fermi sea, generating a rearrange of leptons that liberates an energy equal to the difference between the chemical potential and the target lepton: the Auger energy [24]. An extra contribution comes when the produced lepton is reabsorbed near the surface of the Fermi sea, depositing the excess of energy it had with respect to μ_l : $\Delta E \equiv E_{p_2} - \mu_l$. There is still another contribution that may come from the different masses of the leptons, the target and the produced. However, to keep the thermal distributions in the star, the leptons need to reconvert so that the total number of each species remains constant. Therefore, this contribution is neglected.

INTERACTION RATE OF LFV DARK MATTER

In order to compute the time required by the captured DM particles to thermalize in the center of the star, we need to compute the interaction rate, which follows from Fermi's Golden Rule:

$$\Gamma = 2 \int \mathcal{D}p_{p_1} \mathcal{D}p_{k_2} \mathcal{D}p_{p_2} \frac{\langle |\mathcal{M}|^2 \rangle}{2E_{k_1}} (2\pi)^4 \delta^{(4)}(k_1 + p_1 - k_2 - p_2) n_F(E_{p_1}) (1 - n_F(E_{p_2})), \quad (38)$$

where $\mathcal{D}p \equiv \frac{d^3p}{(2\pi)^3 2E_p}$ and $\langle |\mathcal{M}|^2 \rangle$ is the squared amplitude of the process, summed over all possible final spins and averaged over the initial ones, and it is equal to:

$$\langle |\mathcal{M}|^2 \rangle = \frac{At + Bt^2}{(t - m_a^2)^2}, \quad (39)$$

where $A \equiv -g_{\mu e}^2 g_\chi^2 (m_\mu^2 + m_e^2 - 2m_\mu m_e \cos 2\phi)$ and $B \equiv g_{\mu e}^2 g_\chi^2$. Following [15], we will express Γ as:

$$\Gamma = \int \frac{d^3p_{k_2}}{(2\pi)^3} \frac{\langle |\mathcal{M}|^2 \rangle}{(2E_{k_1})(2E_{k_2})(2m_1)(2m_2)} \Theta(E_{k_2} - m_\chi) \Theta(q_0) S(q_0, q), \quad (40)$$

where the first Θ -function guarantees that the outgoing DM particle has an energy greater than its mass, the second one forces the energy transfer to go from the DM current to the leptonic one (which is demanded by Pauli blocking at $T \rightarrow 0$), $S(q_0, q)$ is expressed in terms of q_0 and q , the time and spatial components of the transverse momentum, so that we can transform the integral in p_{k_2} into those variables. $S(q_0, q)$ is explicitly:

$$\begin{aligned} S(q_0, q) &= 8m_1 m_2 \int \mathcal{D}p_{p_1} \mathcal{D}p_{p_2} (2\pi)^4 \delta^{(4)}(k_1 + p_1 - k_2 - p_2) n_F(E_{p_1}) (1 - n_F(E_{p_1})) \Theta(E_{p_1} - m_1) \Theta(E_{p_2} - m_2) \\ &= \frac{m_1 m_2}{2\pi^2} \int \frac{d^3p_{p_1}}{E_{p_1} E_{p_2}} \delta(q_0 + E_{p_1} - E_{p_2}) n_F(E_{p_1}) (1 - n_F(E_{p_1})) \Theta(E_{p_1} - m_1) \Theta(E_{p_2} - m_2). \end{aligned} \quad (41)$$

We have added again Θ -functions to force the energies to higher values than the masses. After integrating on p_{p_2} with the help of the δ -distribution we can express E_{p_2} in terms of p_{p_1} , q and θ_{q1} , the angle between \vec{q} and \vec{p}_1 :

$$\begin{aligned} E_{p_2} &= \sqrt{m_2^2 + p_{p_1}^2 + q^2 + 2p_{p_1}q \cos \theta_{q1}} \\ &= \sqrt{E_{p_1}^2 + \Delta m_{21}^2 + q^2 + 2p_{p_1}q \cos \theta_{q1}} > m_2, \end{aligned} \quad (42)$$

where $\Delta m_{21}^2 \equiv m_2^2 - m_1^2$. That expression for E_{p_2} goes in the Dirac δ -distribution: $\delta(q_0 + E_{p_1} - E_{p_2}) \rightarrow \delta\left(q_0 + E_{p_1} - \sqrt{E_{p_1}^2 + \Delta m_{21}^2 + q^2 + 2p_{p_1}q \cos \theta_{q1}}\right)$. We can also change the variable p_{p_1} to E_{p_1} by taking into account that $p_{p_1} dp_{p_1} = E_{p_1} dE_{p_1}$, so that: $d^3 p_{p_1} = 2\pi p_{p_1} E_{p_1} dE_{p_1} d\cos \theta_{q1}$, where we took the \hat{z} direction pointing towards \vec{q} .

Now, we can evaluate the Dirac δ by integrating it in $\cos \theta_{q1}$. There are two expressions we need:

1. $\left| \frac{d}{d\cos \theta_{q1}} \left(q_0 + E_{p_1} - \sqrt{E_{p_1}^2 + \Delta m_{21}^2 + q^2 + 2p_{p_1}q \cos \theta_{q1}} \right) \right| = \frac{p_{p_1}q}{E_{p_2}},$
2. $q_0 + E_{p_1} - \sqrt{E_{p_1}^2 + \Delta m_{21}^2 + q^2 + 2p_{p_1}q \cos \theta_{q1}} = 0 \rightarrow \cos \theta_{q1} = \frac{q_0^2 - q^2 + 2q_0 E_{p_1} - \Delta m_{21}^2}{2p_{p_1}q}.$

After replacing these quantities in the expression for $S(q_0, q)$, we obtain:

$$\begin{aligned} S(q_0, q) &= \frac{m_1 m_2}{\pi q} \int dE_{p_1} d\cos \theta_{q1} \delta\left(\cos \theta_{q1} - \frac{q_0^2 - q^2 + 2q_0 E_{p_1} - \Delta m_{21}^2}{2p_{p_1}q}\right) n_F(E_{p_1}) (1 - n_F(E_{p_1})) \Theta(E_{p_1} - m_1) \Theta(E_{p_2} - m_2) \\ &= \frac{m_1 m_2}{\pi q} \int_{m_1}^{\mu} dE_{p_1} \Theta(E_{p_2} - \mu), \end{aligned} \quad (43)$$

where the Fermi distributions were treated for $T \rightarrow 0$, which is a very good approximation for the masses involved, so that the lepton target must have an energy less than the chemical potential, μ , and the outgoing lepton an energy greater than it.

The limits of integration for E_{p_1} need further analysis. We will obtain two more constraints to those limits. First, from the Pauli blocking condition to the outgoing lepton we have: $E_{p_2} = E_{p_1} + q_0 \geq \mu$. Therefore, $E_{p_1} \geq \mu - q_0$. Second, from the condition that the absolute value of the expression found for $\cos \theta_{q1}$ is less or equal than 1, we uncover another condition:

$$\cos^2 \theta_{q1} = \left(\frac{q_0^2 - q^2 + 2q_0 E_{p_1} - \Delta m_{21}^2}{2p_{p_1}q} \right)^2 \leq 1.$$

Therefore:

$$4tE_{p_1}^2 + 4q_0(t - \Delta m_{21}^2)E_{p_1} + 4m_1^2 q^2 + (t - \Delta m_{21}^2)^2 \leq 0,$$

whose roots are:

$$E_{p_1}^{\mp} = -\frac{q_0(t - \Delta m_{21}^2)}{2t} \pm \frac{q\sqrt{(t - \Delta m_{21}^2)^2 - 4m_1^2 t}}{2t}.$$

Taking into account that $t < 0$, the condition for E_{p_1} is:

$$E_{p_1} \leq E_{p_1}^- \vee E_{p_1}^+ \leq E_{p_1}. \quad (44)$$

We need two conditions to be met: (1) $\max(m_1, \mu - q_0) \leq E_{p_1} \leq \mu$ and (2) eq. (44), which will be called region \mathcal{C} . If $I_E(q_0, q)$ is the length of this interval, we have the final expression for $S(q_0, q)$:

$$\begin{aligned} S(q_0, q) &= \frac{m_1 m_2}{\pi q} \int_{\mathcal{C}} dE_{p_1} \Theta(E_{p_2} - \mu) \\ &= \frac{m_1 m_2}{\pi q} I_E(q_0, q) \Theta(E_{p_2} - \mu). \end{aligned} \quad (45)$$

Depending on the point in phase space, the value of $I_E(q_0, q)$ is $[\mu - \max(m_1, \mu - q_0, E_{p_1}^+)] \times \Theta(\mu - E_{p_1}^+) + [\min(E_{p_1}^-, \mu) - \max(m_1, \mu - q_0)] \times \Theta(E_{p_1}^- - \max(m_1, \mu - q_0))$.

Now we need to transform the integral in p_{k_2} into q_0 and q . First, we will express the expression as follows:

$$\Gamma = \frac{1}{64\pi^2 m_1 m_2} \int \frac{p_{k_2}^2 dp_{k_2} d\cos\theta_{k_1 k_2}}{E_{k_1} E_{k_2}} \frac{At + Bt^2}{(t - m_a^2)^2} \Theta(E_{k_2} - m_\chi) \Theta(q_0) S(q_0, q), \quad (46)$$

where $\theta_{k_1 k_2}$ is the angle between \vec{k}_2 and \vec{k}_1 . The relations between the variables are the following:

$$\begin{aligned} p_{k_2} &= \sqrt{(E_{k_1} - q_0)^2 - m_\chi^2} \rightarrow dp_{k_2} = -\frac{(E_{k_1} - q_0)}{p_{k_2}} dq_0, \\ \cos\theta_{k_1 k_2} &= \frac{p_{k_1}^2 + p_{k_2}^2 - q^2}{2p_{k_1} p_{k_2}} \rightarrow d\cos\theta_{k_1 k_2} = -\frac{q}{p_{k_1} p_{k_2}} dq. \end{aligned}$$

With these quantities, we can transform the measure of the integral:

$$dp_{k_2} d\cos\theta_{k_1 k_2} = dq_0 dq \frac{\partial(p_{k_2}, \cos\theta_{k_1 k_2})}{\partial(q_0, q)} = dq_0 dq \frac{E_{k_2} q}{p_{k_1} p_{k_2}^2}. \quad (47)$$

Then, the interaction rate takes the following form:

$$\begin{aligned} \Gamma &= \frac{1}{64\pi^2 m_1 m_2 E_{k_1} p_{k_1}} \int dq_0 dq q \frac{At + Bt^2}{(t - m_a^2)^2} \Theta(E_{k_2} - m_\chi) \Theta(q_0) S(q_0, q) \\ &= \frac{1}{64\pi^3 E_{k_1} p_{k_1}} \int dq_0 dq \frac{At + Bt^2}{(t - m_a^2)^2} I_E(q_0, q) \\ &\quad \times \Theta(E_{k_2} - m_\chi) \Theta(q_0) \Theta(E_{p_2} - \mu), \end{aligned} \quad (48)$$

Now we need to obtain the limits of integration:

$$\cos^2\theta_{k_1 k_2} = \left(\frac{p_{k_1}^2 + (E_{k_1} - q_0)^2 - m_\chi^2 - q^2}{2p_{k_1} \sqrt{(E_{k_1} - q_0)^2 - m_\chi^2}} \right)^2 \leq 1.$$

Therefore:

$$q^4 - 2 \left((E_{k_1} - q_0)^2 - m_\chi^2 + p_{k_1}^2 \right) q^2 + \left((E_{k_1} - q_0)^2 - m_\chi^2 - p_{k_1}^2 \right)^2 \leq 0,$$

whose roots are:

$$q_\pm^2 = \left((E_{k_1} - q_0)^2 - m_\chi^2 + p_{k_1}^2 \right) \pm 2p_{k_1} \sqrt{(E_{k_1} - q_0)^2 - m_\chi^2}.$$

It can be shown that the last expression is equivalent to: $q_\pm^2 = (p_{k_1} \pm p_{k_2})^2$, therefore:

$$p_{k_1} - p_{k_2} \leq q \leq p_{k_1} + p_{k_2}, \quad (49)$$

such that $p_{k_2} = \sqrt{(E_{k_1} - q_0)^2 - m_\chi^2}$. In addition, in the case of q_0 , the limiting values are transferring no energy or all the kinetic energy from the incoming DM particle to the leptonic current. So the final expression for the interaction rate is:

$$\Gamma = \frac{1}{64\pi^3 E_{k_1} p_{k_1}} \int_0^{E_{k_1} - m_\chi} dq_0 \int_{p_{k_1} - \sqrt{(E_{k_1} - q_0)^2 - m_\chi^2}}^{p_{k_1} + \sqrt{(E_{k_1} - q_0)^2 - m_\chi^2}} dq \frac{At + Bt^2}{(t - m_a^2)^2} I_E(q_0, q). \quad (50)$$

In this expression, t needs to be expressed in terms of the integration variables: $t = q_0^2 - q^2$. It is also important to note that, since $q_0 \geq 0$ and all the DM particles have the same mass, $p_{k_1} \geq p_{k_2}$ and it is not necessary to impose the absolute value of $p_{k_1} - p_{k_2}$ in the second integral above. Given the presence of many channels for capturing the DM, we can compute the total interaction rate as the sum of the rate for each channel, Γ_i :

$$\Gamma_{\text{tot}} \equiv \sum_i \Gamma_i. \quad (51)$$

THERMALIZATION AND ANNIHILATION OF LFV DARK MATTER

Thermalization time

General treatment

To find the thermalization time, we need to find the time for each interaction until the mean kinetic energy is equal to $E_f - m_\chi \equiv \frac{3}{2}T_{NS}$, where T_{NS} is the temperature of the star and also the DM in it. The time for each interaction is computed as the inverse of the interaction rate, found in the previous section. The process of computation consists in finding the mean energy lost by the DM particles in each interaction, so that the overall energy can be updated until the kinetic energy reaches its final estimated value, $E_f - m_\chi$. The initial energy is γm_χ .

The mean kinetic energy transferred in an interaction is just the average of q_0 weighted by the interaction rate itself [15]:

$$\langle K \rangle = \frac{1}{\Gamma} \int dq_0 q_0 \frac{d\Gamma}{dq_0} . \quad (52)$$

In our case, in which there is more than one channel of interaction, we compute the average weighted over the interaction rate for each channel:

$$\langle K \rangle = \sum_i \frac{\Gamma_i \times \langle K \rangle_i}{\Gamma_{\text{tot}}} , \quad (53)$$

where $\langle K \rangle_i$ is the mean kinetic energy transferred computed just for one channel. Therefore, for the i -th interaction of a DM particle of energy E_i , the outgoing energy will on average be equal to $E_{i+1} = E_i - \langle K \rangle$. Then, the thermalization time is:

$$\tau_{\text{th}} = \sum_{i=1}^N \frac{1}{\Gamma(E_i)} , \quad (54)$$

such that $E_N \leq E_f < E_{N-1}$, where E_f is the final energy attained by the iterative process.

Inelastic processes subtleties

For usual elastic processes, the procedure described just above can be performed down to any temperature, especially the temperature of the star, which is the relevant one to speak about thermalization. In our case, we have an inelastic process. When the DM particles have lost most of their energy, the process $\chi + l_\alpha \rightarrow \chi + l_\beta$ is simply forbidden when $m_\alpha \neq m_\beta$. An intuitive way to see this is the following: when the kinetic energy is low enough, we may regard the incoming and outgoing DM particles nearly at rest. Then, on the leptonic side of the process, we need a target lepton with an energy $E_{p_1} \lesssim \mu$, while the outgoing energy is $E_{p_2} \gtrsim \mu$. If we impose energy conservation, we cannot achieve momentum conservation, since both particles have different mass.

We can also show this in a more rigorous way. The roots in Equation (44) can be expanded in powers of q and q_0 . We are considering them to be very small, since we are studying the behavior of the conditions for very low temperatures. Their values to first order are

$$E_{p_1}^\pm = \pm \frac{|\Delta m_{\mu e}^2|}{2q} + \mathcal{O}(q^0, q_0^0) , \quad (55)$$

where $\mathcal{O}(q^0, q_0^0)$ means that we are just keeping the poles in a Laurent series expansion. The first term is the one that dominates for small q and q_0 . It is clear that $E_{p_1}^-$ is in this case negative and by setting $E_{p_1}^+ > \mu$, we can be

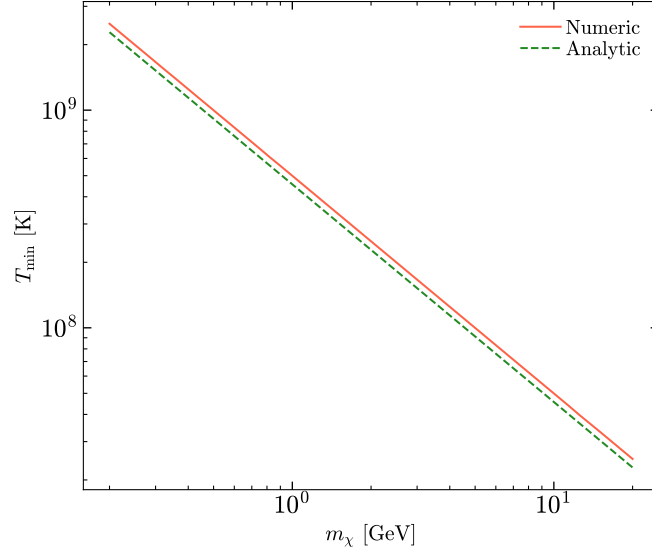


FIG. 4. Lowest temperature reached by DM for case 1 and a NS of mass of $2 M_\odot$ (BSk 25).

sure that there is no available target lepton with that energy. In this way, we freeze the transfer of energy between the DM and the NS. The minimum temperature is attained when $E_{p_1}^+ \simeq \frac{|\Delta m_{\mu e}^2|}{2q} \sim \mu$, therefore, when $q \sim \frac{|\Delta m_{\mu e}^2|}{2\mu}$. As can be seen, the interaction is totally excluded when the maximum value of q , $q_{\max} = p_{k_1} + p_{k_2}$, is excluded. To obtain this limit, we need to consider that the kinetic energy left, K , is related to the temperature: $K = \frac{3}{2}T$. So, if the temperature is really smaller than the mass of the DM, we can approximate $p_{k_1} = \sqrt{3m_\chi T} \simeq p_{k_2}$. Here we are assuming the value of q_0 is negligible, which is actually the case for our Laurent expansion of $E_{p_1}^+$. Therefore, we can express q in terms of the temperature and put it in the limit when any interaction is excluded at three level: $q_{\max} = 2\sqrt{3m_\chi T} \sim \frac{|\Delta m_{\mu e}^2|}{2\mu}$. By applying this approximation, we get a very similar result than performing the whole computation until the temperature DM stabilizes and ceases to decrease, as seen in Figure 4. The minimum value of the temperature is:

$$T_{\min} \simeq \frac{1}{3m_\chi} \left(\frac{\Delta m_{\mu e}^2}{4\mu} \right)^2. \quad (56)$$

Annihilation of DM in the star

Although the DM accumulated in the center of the star cannot reach the temperature of the star, it can still annihilate and contribute in this way to heating the NS. The amount of DM fermions annihilating per time is [23]:

$$\frac{dN_\chi^{\text{ann}}}{dt} = A_\chi N_\chi^2, \quad (57)$$

where A_χ is an annihilation factor that appears in the annihilation rate of DM: $\Gamma_{\text{ann}} = \frac{1}{2} A_\chi N_\chi^2$. It can be approximated as [23]:

$$A_\chi = \frac{\langle \sigma_{\text{ann}} v_\chi \rangle}{N_\chi^2} \int n_\chi^2(r) d^3r \sim \frac{\langle \sigma_{\text{ann}} v_\chi \rangle}{(2\pi)^{3/2} r_0^3}, \quad (58)$$

where σ_{ann} is the annihilation cross section, v_χ is the velocity of the dark matter, n_χ is the DM number density and r_0 is defined from the DM distribution, such that:

$$n_\chi(r) \equiv n_0 e^{-r^2/r_0^2} = n_0 \exp \left[-\frac{m_\chi \Phi(r)}{T_{\text{DM}}} \right], \quad (59)$$

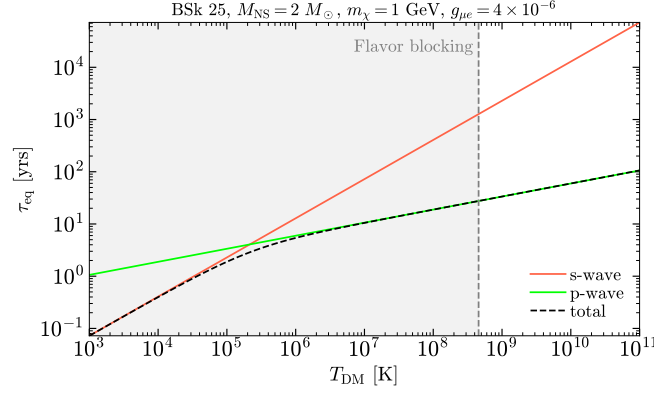


FIG. 5. Equilibration time with respect to each channel and the DM temperature for an NS of mass of $2 M_{\odot}$ (BSk 25) and DM of mass 1 GeV .

where $n_0 = \frac{N_{\chi}}{\pi^{3/2} r_0^3}$ is the DM number density at the center of the star, $\Phi(r) \equiv V(r)/m_{\chi} \simeq \frac{2}{3} \pi G \rho_c r^2$ is the gravitational potential per unit mass at r , ρ_c is the density of the core of the star, G is Newton's gravitational constant, T_{DM} is the DM's temperature, and the second equality follows from considering the virial theorem, such that $\langle K \rangle = \langle V \rangle$. Then, by equating those expression for the DM distribution we obtain,

$$r_0 \sim \sqrt{\frac{3T_{\text{DM}}}{2\pi G m_{\chi} \rho_c}}. \quad (60)$$

We note that the radius of the DM thermosphere can be found from $r_{\text{th}} = \sqrt{\langle r^2 \rangle} = (3/2) \sqrt{T_{\text{DM}}/\pi G m_{\chi} \rho_c} = \sqrt{3/2} r_0$.

We finally need to compute the number of DM particles enclosed in the sphere of radius r_0 . This can be done by considering the full evolution of the number of DM fermions:

$$\frac{dN_{\chi}}{dt} = C - A_{\chi} N_{\chi}^2, \quad (61)$$

where C is the capture rate. Therefore, the total number of particles as a function of time is the solution of the previous equation:

$$N_{\chi}(t) = \sqrt{\frac{C}{A_{\chi}}} \tanh\left(\sqrt{C A_{\chi}} t\right). \quad (62)$$

Therefore, we can now compute the contribution to \dot{E}_k in Equation (6) coming from annihilations, which gives us a total energy rate deposition of:

$$\dot{E}_k^{\text{tot}} = \dot{E}_k + m_{\chi} A_{\chi} N_{\chi}^2. \quad (63)$$

Compared to the age of an old and cold NS, an equilibrium between capture and annihilation is easily attained, such that $C = A_{\chi} N_{\chi}^2$, so that $\dot{E}_k^{\text{tot}} = \dot{E}_k + m_{\chi} C$. This is driven by the p -wave annihilation process, which dominates thanks to the higher temperatures of the DM due to flavor blocking, as can be seen in Figure 5.